CrossMark

TECHNICAL PAPER

A non-ideally excited pendulum controlled by SDRE technique

Angelo Marcelo Tusset[1] · Átila Madureira Bueno[2] · João Paulo Martins dos Santos[3] ·
Masayoshi Tsuchida[4] · José Manoel Balthazar[5]

Abstract   In this work, the perturbation theory is applied
to the analysis of an electromechanical pendulum system.
The frequency response behavior of the system is studied,
and the existence of unstable poles is detected using the
Routh–Hurwitz criterion. Numerical simulations show the
existence of nonlinear behaviors such as hysteresis and the
Sommerfeld effect in the resonance region. To damp the
electromechanical system oscillations due to the nonlinear
characteristics of the system the State Dependent Riccati
Equation (SDRE) technique is used. The SDRE control
strategy is applied considering two control signals, a feed-
back control that force the state trajectory of the system to
a previously defined periodic orbit, and a nonlinear feedfor-
ward control that keeps the system motion synchronized to
the periodic orbit. Additionally, the robustness of the con-
trol technique is tested for parametric uncertainties.

Keywords   Nonlinear control · Non-ideal systems ·
SDRE · Hysteresis · Sommerfeld effect

Technical Editor: Aline Souza de Paula.

✉ Átila Madureira Bueno
    atila@sorocaba.unesp.br

    Angelo Marcelo Tusset
    tusset@utfpr.edu.br

    João Paulo Martins dos Santos
    jp2@usp.br

    Masayoshi Tsuchida
    tsuchida@ibilce.unesp.br

    José Manoel Balthazar
    Josemanoel.balthazar@feb.unesp.br

[1] Departamento Acadêmico de Matemática - DAMAT,
    Universidade Tecnológica Federal do Paraná - UTFPR,
    Ponta Grossa, PR, Brazil

1 Introduction

Usually, the mathematical models of dynamical systems
suppose that the excitation signals[1] are ideal, that is, the
power source is not affected by the dynamical system
behavior. For instance, the frequency of an oscillatory exci-
tation signal is determined by the power source, not
depending on the motion of the dynamical system. This
kind of system is said to have an ideal (unlimited) power
supply.

In the recent decades the interest on non-ideal systems
has grown. In non-ideal systems the excitations signals
have limited power supply, and therefore, the behavior
of the excitation signal is affected by the motion of the
dynamical system. In 1902 the first non-ideal problem
was reported when Sommerfeld observed the interactions
between a motor and its elastic foundation (a cantilever
beam). The system exhibited unstable motions in the reso-
nance region, usually known as jump phenomenon or Som-
merfeld effect [1].

[2] Instituto de Ciência e Tecnologia de Sorocaba - ICTS,
    Universidade Estadual Paulista - UNESP, Sorocaba,
    SP, Brazil

[3] Academia da Força Aérea (AFA), Pirassununga, SP, Brazil

[4] Departamento de Ciência da Computação e Estatística - DCCE,
    Universidade Estadual Paulista - UNESP,
    São José do Rio Preto, SP, Brazil

[5] Divisão de Engenharia Aeronáutica, Instituto Tecnológico de
    Aeronática - ITA, São José dos Campos, SP, Brazil

---

[1] Input signals, forces, or any forcing terms in a differential equation.

🗬 Springer

2460

J Braz. Soc. Mech. Sci. Eng. (2016) 38:2459–2472

According to [3], dynamical systems with non-ideal power sources may develop a number of different behaviors, such as Sommerfeld effect, hysteresis and chaos. The influence on the shape of the response curve when a control parameter is modified is called hysteresis, and the characteristics of the frequency response are sufficient to its characterization [2]. In addition, the Sommerfeld effect can be detected observing the amplitude of the oscillations as a function of the control parameters values [4].

In [5], the observed Sommerfeld effect of a cantilever beam coupled to a non-ideal unbalanced motor is analysed considering numerical and experimental tests. The sensitivity of the system to its parameters variations is determined by numerical simulations.

In [6], the dynamics of a nonlinear oscillator excited by a non-ideal source is studied both numerically and analytically. The Sommerfeld effect was detected by analyzing the amplitude of motion as a function of the excitation frequency. An approach for the parameters determination of the non-ideal system for which the Sommerfeld effect does not exist is developed.

In [7], a feedback control is used to generate chaotic oscillations in a simple electromechanical device, and numerical simulations detected the existence of Sommerfeld effect.

In [8], the Bogoliubov Averaging Method is applied to study the vibrations in an elastic foundation forced by a non-ideal energy source. Considering the equations of motion, numerical simulations, and the averaged equations, the authors conclude that the Bogoliubov averaging method is an excellent tool to study the characteristics of motion of a non-ideal system.

In [9], the nonlinear control method based on the saturation phenomenon is applied to a non-ideal portal frame system. The equations of motion are analyzed using the method of averaging and numerical simulation. The results show that the motion of the portal frame becomes saturated, and most of the energy supplied to the portal frame by the non-ideal source is transferred to the controller.

In [10], a magnetically levitated body excited by a non-ideal energy source is numerically analyzed, and it is observed that the maximum vibration amplitude occurred in the regions where the jump phenomenon occurs. To decrease the amplitude of oscillations on the resonances regions, passive and active controllers are proposed.

In [11], the attenuation and suppression of the Sommerfeld effect in a non-ideal vibrating system using a magnetorheological damper (MRD) is studied. Numerical simulations exhibited different variations of the Sommerfeld effect for different current values applied to the MRD.

In [12], the dynamic behavior and vibration control of an electromechanical system under non-ideal excitation is

studied. The Routh–Hurwitz stability criterion is used to determine the stability of the controlled system.

In this work the motion control of a non-ideally excited pendulum is proposed. Two control strategies are designed, a feedback controller that captures the system motion to a previously defined orbit [13], and a feedforward controller that keeps the system motion synchronized to that orbit. The feedback controller is designed using the State-Dependent Riccati Equation (SDRE) technique.

The SDRE was first proposed by [14], and studied by [15–17], and has become popular over the control community during the last decade. The state transitions in the SDRE method depend on a matrix valued state dependent function. Additionally, the nonlinear terms are parametrized in the state vector. It is an effective algorithm for synthesizing feedback control, considering a nonlinear state space equation, to generate successive optimal solutions for the non-ideal system, being successfully applied to nonlinear systems [13, 18, 19], electromechanical pendulum [20, 21], robotic systems [22–24], micro electro-mechanical systems (MEMS) [25, 26] and atomic force microscopy (AFM) systems [27–30].

2 Mathematical model, derivation of governing equations and approximate analytical solution

The dynamics of an electro-mechanical pendulum with non-ideal power source, shown in Fig. 1, is investigated. The system consists of a mass block m_1 (kg) that oscillates horizontally because of the rotation of the mass m_2 (kg) in a distance R (m) from the DC motor axis. The mass block m_1 is connected to the wall by a spring and a damper, with coefficients k_1 (N/m) and c_1 (Nm/s), respectively. A pendulum of mass m_3 (kg) and length l (m) is joined to the block.

Defining the generalized coordinates by $\begin{pmatrix} q_1 & q_2 & q_3 \end{pmatrix}$, where q_1 is the horizontal displacement of mass m_1, q_2 is the angular displacement of the mass m_2, and q_3 is the angular displacement of the pendulum with mass m_3. The kinetic energy T, the potential energy V, and the external forces $N_i, i = 1, 2, 3$, are given by:

$$T = \frac{1}{2}\left\{ m_1\dot{q}_1^2 - 2m_2R\dot{q}_1\dot{q}_2\sin q_2 + \left(m_2R^2 + J_2 \right)\dot{q}_2^2 \right.$$
$$\left. + 2m_3l\dot{q}_1\dot{q}_3\cos q_3 + m_3l^2\dot{q}_3^2 \right\}$$

$$V = \frac{1}{2}k_1q_1^2 + g\{m_2R\sin q_2 + m_3l(1 - \cos q_3)\}$$

$$N_1 = -c_1\dot{q}_1, \quad N_2 = M(\dot{q}_2) = a - b\dot{q}_2, \quad N_3 = -c_3\dot{q}_3 \tag{1}$$

Applying the Lagrange formulation, the dynamical electro-mechanic pendulum system equations of motion are given by:

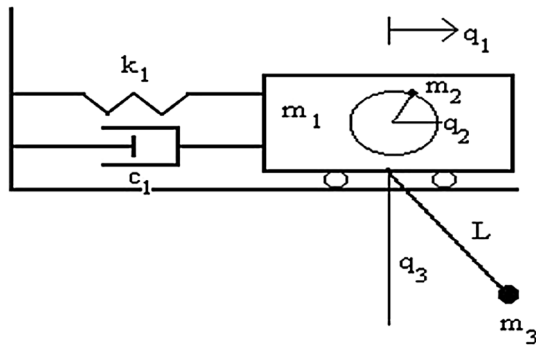**Fig. 1** Electro-mechanical pendulum system

$$m_1\ddot{q}_1 - m_2R\left(\ddot{q}_2\sin q_2 + \dot{q}_2^2\cos q_2\right)$$
$$+ m_3l\left(\ddot{q}_3\cos q_3 - \dot{q}_3^2\sin q_3\right) + k_1q_1 = -c_1\dot{q}_1$$
$$I\ddot{q}_2 - m_2R\dot{q}_1\sin q_2 + gm_2R\cos q_2 = M(\dot{q}_2)$$
$$m_3l^2\ddot{q}_3 + m_3l\ddot{q}_1\cos q_3 + gm_3l\sin q_3 = -c_3\dot{q}_3 \quad (2)$$

given that $I = m_2R^2 + J_2$, where J_2 is the rotor moment of inertia.

The function $M(\dot{q}_2)$ is the driving torque of the motor, and according to [31], the inductance value is much smaller than the response time constant of the system, and therefore, in the steady state it can be considered that $M(\dot{q}_2) = a - b\dot{q}_2$, where a is related to the voltage applied across the armature of the DC motor, and b is constant for the considered DC motor.

The friction force on the mass m_1 is given by $N_1 = -c_1\dot{q}_1$, and the friction on the pendulum is given by $N_3 = -c_3\dot{q}_3$, and g is the acceleration due to gravity.

In the following, the method of variation of parameters is applied to obtain an approximate solution of the system. To that, the new dimensionless variables are defined by: $\tau = \omega t$, $u = \frac{q_1}{l}$, $\varphi = \frac{q_2}{Q_2}$ and $\theta = \frac{q_3}{Q_3}$ with $\omega^2 = \frac{k_1}{m_1}$, where l [m], $Q_2 = 1$ [rad] and $Q_3 = 1$ [rad] are constants, and the dimensionless equations of motion are given by:

$$u'' = -\varepsilon\mu_1u' - u + \varepsilon p_2\varphi''\sin(\varphi) + \varepsilon p_2\varphi'^2\cos(\varphi)$$
$$\quad - \varepsilon p_5\theta'^2\theta + \varepsilon p_5\theta''$$
$$\theta'' = -\varepsilon\mu_3\theta' - \omega_3^2\theta - u''$$
$$\varphi'' = \varepsilon\alpha - \varepsilon\beta\varphi' + \varepsilon p_3u''\sin(\varphi) - \frac{\varepsilon p_4g}{\omega^2}\cos(\varphi) \quad (3)$$

given that $m = m_1 + m_2 + m_3$, $\frac{c_1}{m\omega} = \varepsilon\mu_1$, $\omega_3^2 = \frac{g}{l\omega^2}$, $\frac{m_2R}{ml} = \varepsilon p_2$, $\frac{m_2Rl}{I} = \varepsilon p_3$, $\frac{m_2R}{I} = \varepsilon p_4$, $\frac{a}{\omega^2} = \varepsilon\alpha$, $\frac{b}{\omega} = \varepsilon\beta$, $\frac{c_1}{m\omega} = \varepsilon\mu_1$, $\frac{c_3}{m_3l^2\omega} = \varepsilon\mu_3$, $\frac{m_3}{m} = \varepsilon p_5$, $\omega_1^2 = \frac{k_1}{m_1}$, $\omega_1 - \Omega = \varepsilon\sigma_\Omega$, $\frac{M(\dot{q}_2)}{\omega^2 I} = \varepsilon M_1(\varphi')$, $M_1(\dot{\varphi}) = \alpha - \beta\varphi'$, where $0 < \varepsilon << 1$ is an arbitrary small parameter. Additionally, for small displacements $\sin(\theta) = \theta$ and

$\cos(\theta) = 1$. The dimensionless time τ derivative is denoted by $\frac{dy}{d\tau} = y'$, and σ_Ω is a detuning parameter [23].

For $\varepsilon \approx 0$ results that:

$$u'' = -u$$
$$\theta'' = -\omega_3^2\theta - u''$$
$$\varphi'' = 0 \quad (4)$$

Solving Eq. (4) it can be noted that the motor rotates with constant angular frequency $\varphi' = \Omega$. The mass block moves harmonically with frequency $\omega_1 = 1$. The pendulum describes a forced movement, and the force is periodically excited with frequency ω_1, resulting that:

$$u = a_1\cos(\omega_1\tau + \beta_1)$$
$$u' = -a_1\omega_1\sin(\omega_1\tau + \beta_1)$$
$$\theta = a_3\cos(\omega_3\tau + \beta_3) + a_1\delta\cos(\omega_1\tau + \beta_1)$$
$$\theta' = -a_3\omega_3\sin(\omega_3\tau + \beta_3) - a_1\omega_1\delta\sin(\omega_1\tau + \beta_1) \quad (5)$$
$$\varphi = \Omega\tau$$
$$\varphi' = \Omega$$

where $\delta = \frac{1}{\omega_3^2 - 1}$.

For $\varepsilon \neq 0$, one can expect the oscillation frequency of the mass block to be approximately harmonic, and the angular frequency φ' to be approximately constant, i.e., the motion correspond to functions that vary smoothly over time, and, in this case, the block oscillation is governed by the motor speed. Furthermore, in the presence of dissipative terms the oscillation is forced, and since the θ varies smoothly over time, it depends on the oscillation amplitude and phase of the block movement. Thus an approximate for (5) [2, 6, 9, 31] is given by:

$$u = a_1\cos(\varphi + \beta_1)$$
$$\theta = a_3\cos(\omega_3\tau + \beta_3) + a_1\delta\cos(\varphi + \beta_1) \quad (6)$$

$$u' = -a_1\Omega\sin(\varphi + \beta_1)$$
$$\theta' = -a_3\omega_3\sin(\omega_3\tau + \beta_3) - a_1\Omega\delta\sin(\varphi + \beta_1) \quad (7)$$

$$\varphi = \Omega\tau$$
$$\varphi' = \Omega \quad (8)$$

Considering $a_1 = a_1(\tau)$, $\beta_1 = \beta_1(\tau)$, $a_3 = a_3(\tau)$, $\beta_3 = \beta_3(\tau)$ and $\Omega = \Omega(\tau)$, the set of variables $(a_1, \beta_1, a_3, \beta_3, \Omega)$, smoothly varying over τ, represent the essential parameters of the system [1]. The values of the essential variables are determined by the method of averaging [2]. Consequently, considering the derivative of the Eq. (6) with respect to τ, results:

$$u' = a_1'\cos(\varphi + \beta_1) - a_1(\Omega + \beta_1')\sin(\varphi + \beta_1)$$
$$\theta' = a_3'\cos(\omega_3\tau + \beta_3) - a_3(\omega_3 + \beta_3')\sin(\omega_3\tau + \beta_3)$$
$$\quad + a_1'\delta\cos(\varphi + \beta_1) - a_1\delta(\Omega + \beta_1')\sin(\varphi + \beta_1) \quad (9)$$

From Eqs. (5)–(9) we have:

2462

J Braz. Soc. Mech. Sci. Eng. (2016) 38:2459–2472

$$a_1' \cos(\varphi + \beta_1) - a_1 \beta_1' \sin(\varphi + \beta_1)$$
$$- (\Omega - \omega_1)a_1 \sin(\varphi + \beta_1) = 0$$
$$a_3' \cos(\omega_3\tau + \beta_3) - a_3\beta_3' \sin(\omega_3\tau + \beta_3) = 0 \quad (10)$$

The derivative of Eq. (7) with respect to τ is given by:

$$u'' = -a_1'\omega_1 \sin(\varphi + \beta_1) - a_1\omega_1(\Omega + \beta_1')\cos(\varphi + \beta_1)$$
$$\theta'' = -a_3'\omega_3 \sin(\omega_3\tau + \beta_3) - a_3\omega_3(\omega_3 + \beta_3')\cos(\omega_3\tau + \beta_3)$$
$$- a_1'\delta\omega_1 \sin(\varphi + \beta_1) - a_1\delta\omega_1(\Omega + \beta_1')\cos(\varphi + \beta_1) \quad (11)$$

Replacing Eqs. (6), (8) and (9) into Eq. (3), and comparing with (11), results:

$$- a_1'\gamma \sin(\varphi + \beta_1) - a_1\beta_1'\gamma_1 \cos(\varphi + \beta_1)$$
$$+ \left(\omega_1^2 - \gamma_1\Omega\right)a_1 \cos(\varphi + \beta_1) = \varepsilon[H]$$

$$\Omega' = \varepsilon \left\{ \begin{array}{l} M_1(\Omega) - p_3 \sin(\varphi)\left[a'\omega_1 \sin(\varphi + \beta_1)\right. \\ + a_1\beta_1'\omega_1 \cos(\varphi + \beta_1) + a_1\omega_1\Omega \cos(\varphi + \beta_1)] \\ - p_4\dfrac{g}{\omega^2} \cos(\varphi) \end{array} \right\}$$

$$- a_3'\omega_3 \sin(\omega_3\tau + \beta_3) - a_3\omega_3\beta_3' - \cos(\omega_3\tau + \beta_3) = [J] \quad (12)$$

where $\gamma_1 = \left(1 + \varepsilon p_5 \delta\omega_1^2\right)$, $\gamma = (1 + \varepsilon p_5)$, and

$$[H] = \left[p_2\Omega' \sin(\varphi) + p_2\Omega^2 \cos(\varphi)\right.$$
$$\left. + \mu_1 a_1\omega_1 \sin(\varphi + \beta_1)\right] + m_3[G]$$

$$[G] = [a_3\omega_3 \sin(\omega_3\tau + \beta_3) + a_1\delta\omega_1 \sin(\varphi + \beta_1)]^2$$
$$\times [a_3 \cos(\omega_3\tau + \beta_3) + a_1\delta \cos(\varphi + \beta_1)]$$
$$+ a_3'\omega_3 \sin(\omega_3\tau + \beta_3) + a_3\omega_3\beta_3' \cos(\varphi + \beta_1)$$
$$+ a_3\omega_3^2 \cos(\omega_3\tau + \beta_3)$$

$$[J] = -a_1\omega_1 \sin(\varphi + \beta_1) - a_1\beta_1'\omega_1 \cos(\varphi + \beta_1)$$
$$+ \varepsilon\mu_3[a_3\omega_3 \sin(\omega_3\tau + \beta_3) + a_1\delta\omega_1 \sin(\varphi + \beta_1)]$$
$$+ \delta\omega_1\left[a_1' \sin(\varphi + \beta_1) + a_1\beta_1' \cos(\varphi + \beta_1)\right]$$
$$+ a_1\delta\left[\omega_1\Omega - \omega_3^2\right] \cos(\varphi + \beta_1) \quad (13)$$

Considering the following trigonometric identities:

$$\sin^2(\theta) = \frac{1}{2} - \frac{1}{2} \cos(2\theta)$$
$$\sin^4(\theta) = \frac{1}{8}(\cos(4\theta) - 4\cos(2\theta) + 3)$$
$$\sin^3(\theta) \cos(\theta) = \frac{1}{8}(2\sin(2\theta) - \sin(4\theta))$$
$$\cos^4(\theta) = \frac{1}{8}(\cos(4\theta) + 4\cos(2\theta) + 3)$$
$$\cos^3(\theta) \sin(\theta) = \frac{1}{8}(2\sin(2\theta) + \sin(4\theta)) \quad (14)$$

and solving Eqs. (10) and (12) for a_1', β_1', Ω', a_3' and β_3', the modulations of amplitude and phase of the system are given by [2]:

$$a_1' = -\varepsilon\frac{p_5\delta\omega_1^2 a_1}{2\gamma_1} \sin[2(\varphi + \beta_1)] - \frac{\varepsilon}{\gamma_1}$$
$$\times \left[p_2\Omega^2 \cos(\varphi) + \mu_1 a_1\omega_1 \sin(\varphi + \beta_1)\right] \sin(\varphi + \beta_1)$$
$$- \varepsilon\frac{p_5}{\gamma_1} \sum_{i=1}^{14} G_i + O(\varepsilon^2)$$

$$\beta_1' = -\Omega + \frac{\omega_1^2}{\gamma_1} + \frac{\varepsilon p_5\delta\omega_1^2}{2\gamma_1}\left\{1 - \cos[2(\varphi + \beta_1)]\right\}$$
$$- \frac{\varepsilon \cos(\varphi + \beta_1)}{\gamma_1 a_1} \times \left[p_2\Omega^2 \cos(\varphi) + \mu_1 a_1\omega_1 \sin(\varphi + \beta_1)\right]$$
$$- \frac{\varepsilon p_5}{\gamma_1 a_1} \sum_{k=1}^{10} G_k' + O(\varepsilon^2)$$

$$\Omega' = \varepsilon\left[M_1(\Omega) - p_3 a_1\omega_1\Omega \cos(\varphi + \beta_1) \sin(\varphi) - \frac{p_4 g \cos(\varphi)}{\omega^2}\right]$$
$$+ O\left(\varepsilon^2\right)$$

$$a_3' = \sum_{i=1}^{7} J_i$$
$$\beta_3' = \sum_{k=1}^{8} J_k \quad (15)$$

where G_i, G_k', J_i and J_k depend on sines and/or cosines with frequency, phases and amplitudes determined by an algebraic expansion (see Appendix).

Introducing the detuning parameter to express the difference of the rotation frequency of the motor with the oscillation frequency of the block, $\Omega = 1 + \varepsilon\sigma_\Omega$ [31], results:

$$-\Omega + \frac{\omega_1^2}{\gamma} = -\frac{\varepsilon(\sigma_\Omega + p_5\delta)}{\gamma} + O\left(\varepsilon^2\right) \quad (16)$$

Given that the sine and cosine functions are limited, and a_1', β_1', a_3', β_3', Ω are functions of order ε, ε being a small parameter, then the functions slowly vary over τ, and can be considered constants in the interval $[0, 2\pi]$ [2].

According to Nayfeh [2] there are two ways of doing the calculus of the average. The first is to calculate the average of the Eq. (15) over a period of the circular functions, to determinate a first approximation. In the second method, only the terms of slow variation are kept, and to the first approximation, the average of the equations are considered to be the slow varying terms. In this work, the second method is adopted, and the case without resonance between the block and the pendulum, but with primary resonant interaction between the pendulum and the motor is analyzed. Nayfeh [2] referred this condition is his studies as the non-resonant case.

Considering the system far from the resonance, there will be a resonant interaction only between the block and the motor. Averaging the Eq. (15), the system that describes the behavior of the system far from the resonance, is obtained.

$$a_1' = -\frac{\varepsilon}{2\gamma}\left(p_2\Omega^2 \sin\beta_1 + \mu_1 a_1\right)$$

$$\beta_1' = -\varepsilon\frac{(a_1 + p_5\delta)}{\gamma} + \varepsilon\frac{p_5\delta\omega_1}{2\gamma} - \varepsilon\frac{p_2\Omega^2}{2\gamma a_1}\cos\beta_1 - \frac{\varepsilon p_5}{2\gamma a_1}$$
$$\times\left(\frac{a_3^2\omega_3 a_1\delta}{2} + \frac{a_3^3\omega_1^2\delta^3}{2} - \frac{a_1^3\omega_1^2\delta^3}{4}\right)$$

$$\Omega' = \varepsilon\left[M_1(\Omega) - \frac{1}{2}p_3 a_1\omega_1\Omega\sin(-\beta_1)\right]$$

$$a_3' = -\varepsilon\frac{\mu_3 a_3}{2}$$

$$\beta_3' = 0 \tag{17}$$

To determine the responses of the steady states, there is no need to integrate numerically the set of averaged equations describing the amplitudes and phases of the system. Instead, it is considered that a_1, β_1, a_3, β_3 and Ω are constants in the steady state and, then, the derivatives that describe the modulations of amplitude and phase are null [2], resulting in the following set of algebraic equations:

$$-\frac{\varepsilon}{2\gamma}\left[p_2\Omega^2\sin(\beta_1) + \mu_1 a_1\right] = 0$$

$$-\frac{\varepsilon(\alpha_1 + p_5\delta)}{\gamma} + \frac{\varepsilon p_5\delta\omega_1}{2\gamma}$$
$$-\frac{\varepsilon p_2\Omega^2}{2\gamma a_1}\cos(\beta_1) - \frac{\varepsilon p_5}{2\gamma a_1}\left(\frac{a_3^2\omega_3 a_1\delta}{2} + \frac{a_3^3\omega_1^2\delta^3}{2} - \frac{a_1^3\omega_1^2\delta^3}{4}\right) = 0$$

$$\varepsilon\left[M_1(\Omega) - p_3 a_1\omega_1\Omega\frac{1}{2}\sin(-\beta_1)\right] = 0$$

$$-\varepsilon\frac{\mu_3 a_3}{2} = 0 \tag{18}$$

Taking into account the fourth equation and combining the first and the second equations in (18) yields:

$$\left[\mu_1^2 + \left(2\sigma + p_5\delta - \frac{p_5\delta^3 a_1^2}{4}\right)^2\right]a_1^2 = \left(p_2\Omega^2\right)^2 \tag{19}$$

Combining the first and the third equations yields:

$$M_1(\Omega) - \frac{p_3\mu_1 a_1^2}{2p_2\Omega} = 0 \tag{20}$$

The amplitude of the electro-mechanic pendulum motion, and the rotational frequency of the motor are determined from (19) and (20), respectively, for each value of the control parameter Ω [32]. Additionally, the phase of motion in the steady-state response is given by:

$$\tan(\beta_1) = -\frac{\mu_1}{2\left(\frac{p_5\delta^3 a_1^2}{8} - 2\sigma - p_5\delta\right)} \tag{21}$$

The Eq. (12) is similar to the equation obtained and analyzed by [32] using the multiple scales method, and the averaging method. To determinate the stability of the steady states a_{1c}, β_{1c}, a_{3c}, β_{3c} and Ω_c, the same technique of [32] is applied, considering only the first four equations in (18), and introducing a small perturbation, yielding:

$$a_1 = a_{1c} + \varepsilon A_1; \beta_1 = \beta_{1c} + \varepsilon B_1;$$
$$a_3 = a_{3c} + \varepsilon A_3; \Omega = \Omega_c + \varepsilon\Omega_1 \tag{22}$$

Replacing the small perturbations in the system and expanding in Taylor series around the stationary states, and keeping only the linear terms, results:

$$\mathbf{Y}' = \mathbf{J}|_{\mathbf{Y}_*}\mathbf{Y} \tag{23}$$

where $\mathbf{Y} = \begin{bmatrix} \Omega_1 & A_1 & B_1 & A_3 \end{bmatrix}^T$, $\mathbf{Y}^* = \begin{bmatrix} \Omega_c & a_{1d} & \beta_{1c} & a_{3c} \end{bmatrix}^T$. The Jacobian matrix $\mathbf{J} = \begin{bmatrix} b_{ij} \end{bmatrix}$ is given by:

$$\mathbf{J} = \begin{bmatrix} \varepsilon\left(N - \frac{p_3\mu_1 a_{1c}^2}{2p_2\Omega_c^2}\right) & -\varepsilon\left(\frac{p_3\mu_1 a_{1c}}{2p_2\Omega_c}\right) & b_{13} & 0 \\ \frac{\varepsilon\mu_1 a_{1c}}{\gamma\Omega_c} & \frac{-\varepsilon\mu_1}{2\gamma} & b_{23} & 0 \\ b_{31} & b_{32} & \frac{-\varepsilon\mu_1}{2\gamma} & b_{34} \\ 0 & 0 & 0 & \frac{-\varepsilon\mu_3}{2} \end{bmatrix} \tag{24}$$

With $b_{13} = -\varepsilon\frac{p_3 a_{1c}}{p_2}\left[\left(\sigma_\Omega + \frac{p_5\delta}{2}\right)\frac{a_1}{\Omega} + \frac{p_5\delta_2}{2\Omega_c}\right]$,

$$b_{23} = \frac{\varepsilon a_{1c}}{\gamma}\left[\left(\sigma_\Omega + \frac{p_5\delta}{2}\right) + \frac{p_5\delta_2}{2a_{1c}}\right],$$

$$b_{31} = \frac{2\varepsilon}{\gamma a_{1c}}\left[\left(\sigma_\Omega + \frac{p_5\delta}{2}\right)\frac{a_{1c}}{\sigma_\Omega} + \frac{p_5\delta_2}{2\sigma_\Omega}\right],$$

$$b_{32} = \frac{-\varepsilon}{\gamma a_{1c}}\left[\left(\sigma_\Omega + \frac{p_5\delta}{2}\right) + \frac{p_5}{2}\frac{\partial}{\partial a_{1c}}(\delta_2)\right],$$

$$b_{34} = \frac{-\varepsilon p_5}{2\gamma a_{1c}}\left(a_{3c}\omega_3\delta a_{1c} + \frac{3a_{3c}^2\delta^3}{2}\right), N = \frac{\partial}{\partial\Omega}(M_1(\Omega)),$$ and

$$\delta_2 = \left(\frac{a_{3c}^2\omega_3 a_{1c}\delta}{2} + \frac{a_{3c}^3\delta^3}{2} - \frac{a_{1c}^3\delta^3}{4}\right).$$

The roots of the characteristic polynomial are given by:

$$\left(\varepsilon\frac{\mu_3}{2} + \lambda\right)\left(\lambda^3 - S_1\lambda^2 + S_2\lambda - S_3\right) = 0 \tag{25}$$

where

$$S_1 = b_{11} + b_{22} + b_{33}$$
$$S_2 = (b_{22}b_{33} - b_{32}b_{23})$$
$$\quad + (b_{11}b_{33} - b_{13}b_{31}) + (b_{11}b_{22} - b_{12}b_{21})$$
$$S_3 = \det(\mathbf{J}) \tag{26}$$

According to the Routh–Hurwitz criterion [33], the necessary and sufficient conditions to the roots of the polynomial to have negative real parts, are: $-S_1 > 0$; $-S_3 > 0$; $S_1 S_2 - S_3 > 0$. These conditions are used to obtain the number of eigenvalues with positive real parts.

2464

J Braz. Soc. Mech. Sci. Eng. (2016) 38:2459–2472

3 Steady state

In this section the dynamical system is analyzed considering different control parameters, curves with hysteresis effect, curves of hardening and softening types and jumps in the amplitudes of the motions, are obtained.

3.1 Parameter of control: frequency Ω of the motor rotation

Considering Ω as a control parameter, Eq. (19) is an implicit equation of the amplitude a_1 and a function of the angular frequency Ω. Figure 2b shows the characteristic curve for $a = 0.05$, $b = 0.12$, $m_1 = 3.850$ (kg), $m_2 = 0.008532$ (kg), $m_3 = 0.5$ (kg), $l = 1.19$ (m), $R = 0.075$ (m), $c_1 = 0.0008622$ (Nm/s), $c_3 = 0.3234$ (Nm/s), $k_1 = 1.75$ (N/m), $\sigma = -0.00099$, $\Omega_1 = 0.1$, $\Omega_f = 55.4$, $a_3 = 0.009$, $J_2 = 0.37$ (kg m^2). This diagram shows the stable and unstable stationary states for the averaging Eq. (17).

The stable stationary states are $0 {^\wedge} \Omega_{c1}$ and $\Omega_{c2}^{\wedge} \Omega_c$, and the unstable stationary states are $\Omega_{c1}^{\wedge} \Omega_{c2}$ and for $\Omega > 45.16$. In $\Omega_{c1}^{\wedge} \Omega_{c2}$ the instability is due to the appearance of a positive eigenvalue for $\Omega = 9.97$ and for $\Omega > 19.72$. For $\Omega = 45.16$ the instability is due to the appearing of two eigenvalues with positives real parts.

According to [2], the characteristics of the curve of frequency–response are sufficient to characterize the jump effect, that is, in the points where the tangent of a curve become vertical, and a jump in the amplitude of the movements occur.

More precisely, the amplitude of the oscillations increase over the control parameter Ω, reaching a critical value Ω_{c1}, shown in Fig. 2a. For $\Omega = 19.72$ there is a jump in the amplitude of oscillation, see point 1, and continue to follow up until reach the point $\Omega > 45.16$, where the system becomes unstable due to the appearance of two eigenvalues with positive real parts.

On the other side, following the decreasing direction of Ω, the system is unstable $\Omega > 45.16$, and for $\Omega < 45.16$ the oscillation amplitude of the block decreases until reaching $\Omega = \Omega_{c2}$, where the system experiments a new jump to the point 2 shown in Fig. 2a and, continues softly decreasing until reaching $\Omega = 0$.

For $8.97 < \Omega < 19.72$, the frequency–response curve depends on whether Ω is increasing or decreasing. This phenomenon is called hysteresis [2].

It can be noticed that the system is strongly dependent on the power source dynamics. For $b = 0.07$ the system becomes unstable behavior at the point $\Omega = 27.61$ (Fig. 2b). When $b = 0.02$ the system becomes unstabe for $\Omega = 13.19$ (Fig. 2c).

Forced oscillations are possible only if Eq. (13) is satisfied. In Fig. 2d it can be seen that for a given amplitude of oscillations, up to three roots can be found [1].

Additional modifications on the power source characteristics and on the torque parameters, for example, for $a = 0.03$ and $b = 0.001$, generates much more complex behaviors, indicating the need for further studies to explain the electro-mechanical pendulum system dynamics.

3.2 Control parameter: detuning parameter σ_Ω, and $\delta > 0$

Considering σ_Ω as a control parameter, the curves with softening and hardening characteristics are obtained, depending on whether δ is positive or negative. For $\delta > 0$, the curve is hardening, otherwise, the curve is softening.

In Fig. 3, the characteristics curves are presented for: $m_1 = 3.30$ (kg), $m_2 = 0.002$ (kg), $m_3 = 0.15$ (kg), $l = 1.19$ (m), $R = 0.075$ (m), $c_1 = 0.000898622$ (Nm/s), $c_3 = 0.234$ (Nm/s), $k_1 = 2.2$ (N/m), $\sigma_{\Omega_0} = -0.004$, $\sigma_{\Omega_f} = 0.0015$, $a_3 = 0.09$, $a = 0.01$, $b = 0.0009$, and $J_2 = 0.37$ (kg m^2).

In Figs. 3a, b and 4c the cases for $\Omega = 25.3$, $\Omega = 10.725$ and $\Omega = 9.75$, are respectively shown. In Fig. 3b the instability region is due to a positive eigenvalue, while in Fig. 3c a region of jump in the amplitudes of motion is shown.

3.3 Control parameter: detuning parameter σ_Ω, and $\delta < 0$

For $\delta < 0$ Fig. 4 represents a characteristic curve for the control parameter σ_Ω and $m_1 = 1.30$ (kg), $m_2 = 0.01$ (kg), $m_3 = 0.3$ (kg), $l = 1.19$ (m), $R = 0.075$ (m), $c_1 = 0.8622$ (Nm/s), $c_3 = 1.3234$ (Nm/s), $k_1 = 35.2$ (N/m), $\sigma_0 = -0.5$, $\sigma_f = 0.8$, $a_3 = 0.09$, $a = 0.19$, $b = 0.00051$, $J_2 = 0.4$ (kg m^2).

Figure 4a–c show the cases for $\Omega = 25.3$, $\Omega = 18$ and $\Omega = 17$, respectively. In Fig. 4b, the unstable points on the left side are due to two positive eigenvalues, and the unstable points on the right side are due to a positive eigenvalue. The jump effect can be seen in Fig. 4c.

The jump phenomenon is characterized by a sudden amplitude transition, as indicated in Figs. 3c and 4c. This happens because there is not enough damping in the system to stop the DC motor from transmitting large amounts of energy to the nonlinear oscillator [11].

In Figs. 3 and 4 the influence of parameter (δ) in the curve type ("softening or hardening") can be observed. Similar results were obtained for the non-ideal model in [1].

Non-ideal sources present a strong dependence on the energy supply characteristics, and small changes in the power supply, imply modifications on the stability characteristics of the system. This behavior can be seen
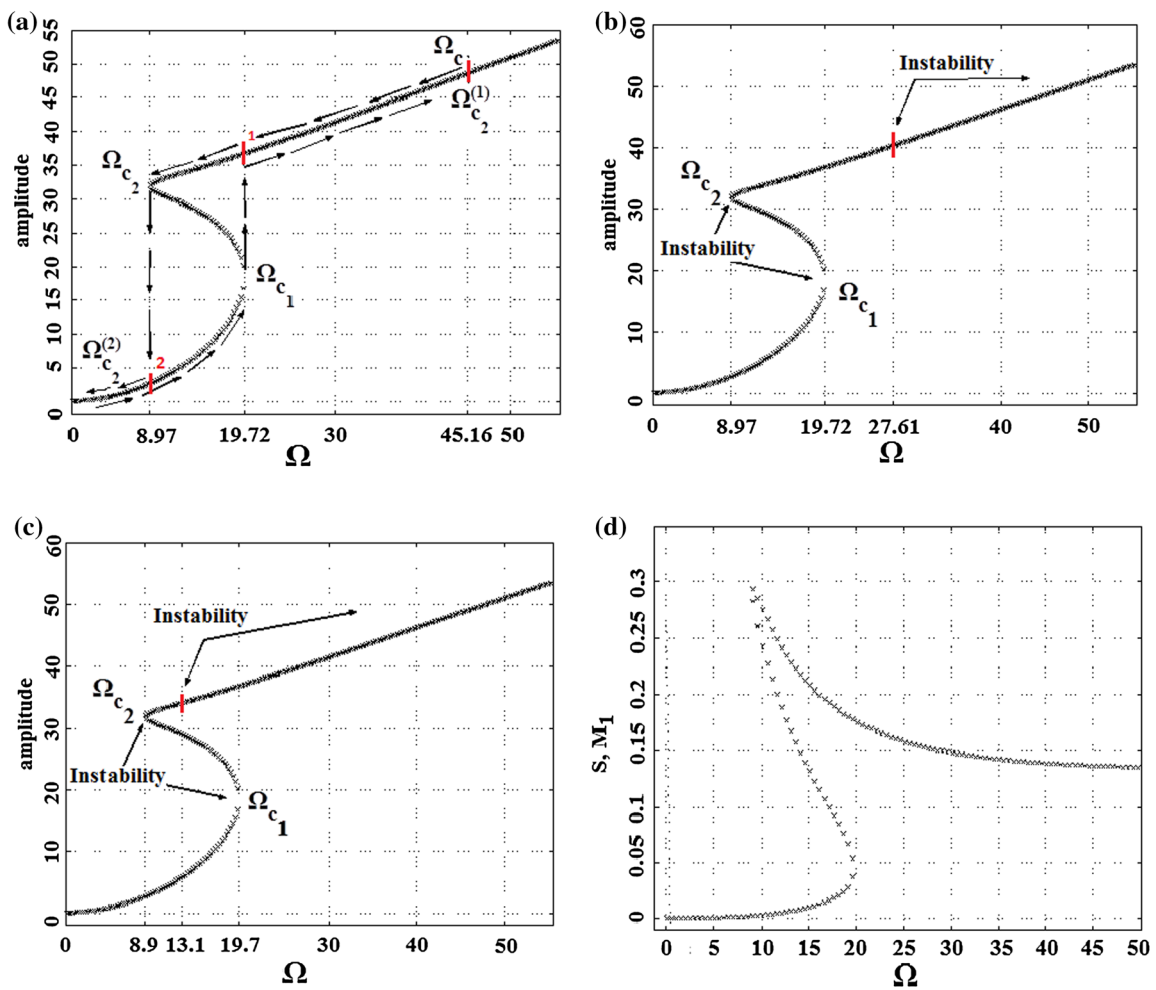
Fig. 2 **a** Frequency–response curve and hysteresis phenomenon, b = 0.12. **b** Unstable and stable points for $b = 0.07$. **c** Unstable and stable points for $b = 0.02$. **d** Intersection of the curves $S(\Omega)$ and linear torque $M_1(\Omega)$

in Figs. 2b, c, 3b and 4b. Figures 2b, c, 3b and 4b show unstable points for variations of the control parameter (Ω) and (σ_Ω), whereas Figs. 3c and 4c show that the jumps in the achievable amplitude movements do not occur near the vertical axis, making evident the effects of non-ideal source on the system behavior [1, 8–12, 31].

In Fig. 5 a comparison of the system (3) and its approximation by average method (Eqs. (6) and (7)) is shown, considering $a = 0.05$, $b = 0.12$, $m_1 = 3.850$ (kg), $m_2 = 0.008532$ (kg), $m_3 = 0.5$ (kg), $l = 1.19$ (m), $R = 0.075$ (m), $c_1 = 0.0008622$ (Nm/s), $c_3 = 0.3234$ (Nm/s), $k_1 = 1.75$ (N/m), $\sigma = -0.00099$, $\Omega_1 = 0.1$, $\Omega_f = 55.4$, $a_3 = 0.009$, $J_2 = 0.37$ (kg m²), $a_1 = 1.1$, $a_3 = 0$, $\beta_1 = -0.1629\tau$, $\beta_3 = 0$, $\Omega = 0.7416$ and $\delta = 0.0513$.

4 Application of the SDRE control

To control u, u', θ and θ', forcing the system to the orbit of Eq. (6), the variables φ and *hedynamicalelectro−mechanicpendulumsystemequa* are considered as disturbances. Then, the dynamic system defined of Eq. (3) can be parameterized as a first order state space equation, written in the state-dependent coefficient (SDC) and non-state-dependent coefficient:

$$\mathbf{x}' = \mathbf{A_x}\mathbf{x} + \mathbf{B}\mathbf{U} + \mathbf{F}(x_i) \qquad (27)$$

where $\mathbf{x} = \begin{bmatrix} x_1 & x_2 & x_2 & x_3 \end{bmatrix}^T$ is the state vector, $\mathbf{x}'$ is the vector of the first order derivatives. $\mathbf{U} = \begin{bmatrix} 0 & u_{sf1} + \tilde{u}_{s1} & 0 & u_{sf2} + \tilde{u}_{s2} \end{bmatrix}^T$, where $\mathbf{u}_{sf}$ is the
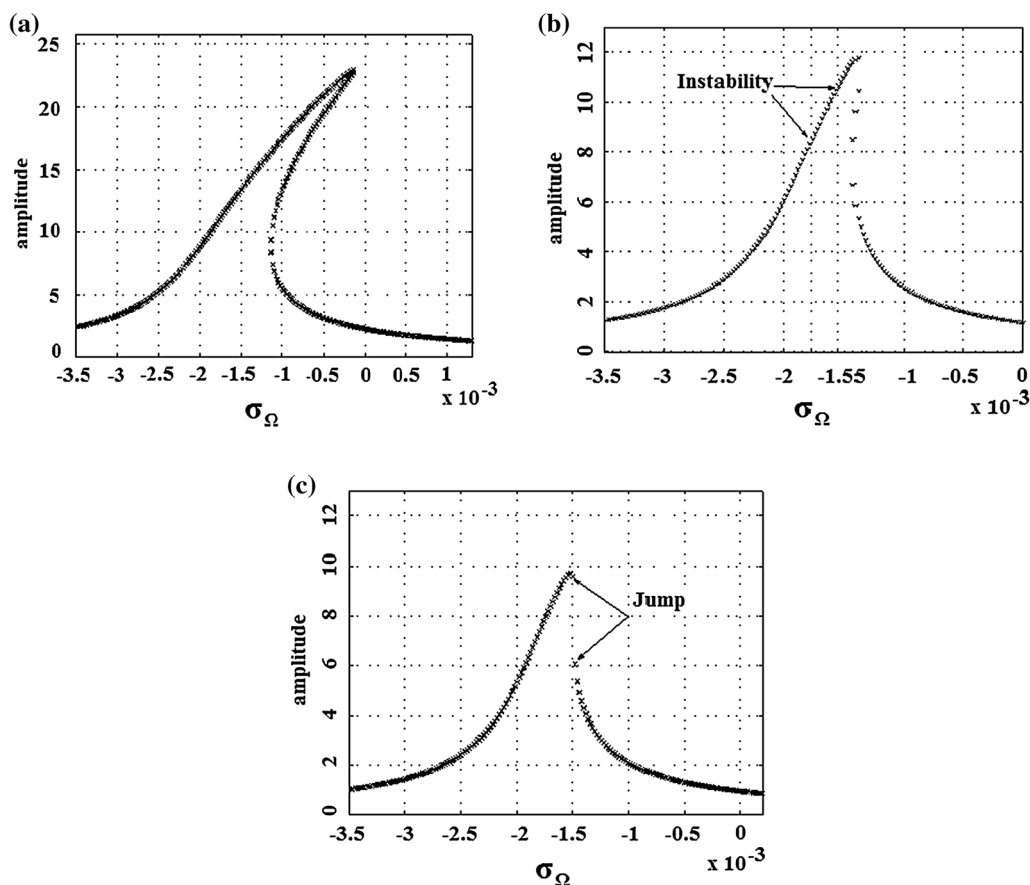
Fig. 3 Frequency–response curve as a function of the control parameter σ_Ω and $\delta > 0$. **a** Frequency- response curve for $\delta > 0$ and $\Omega = 25.3$. **b** Frequency–response curve for $\delta > 0$ and $\Omega = 10.725$. **c** Frequency–response curve with $\delta > 0$ and $\Omega = 9.75$

feedback control signal, $\tilde{\mathbf{u}}_s$ is the feedforward control signal, and $\boldsymbol{F}$ is the nonlinear vector, $i = 1, 2, \ldots, 6$, $x_1 = u$, $x_2 = u'$, $x_3 = \theta$, $x_4 = \theta'$, $x_5 = \varphi$ and $x_6 = \varphi'$.

Considering the system of Eq. (3) written in the form of Eq. (27), results:

$$\mathbf{A_x} = \begin{bmatrix} 0 & 1 & 0 & 0 \\ -\Phi & -\Phi\varepsilon\mu_1 & -\Phi\varepsilon p_5(\omega_3^2 + x_4^2) & -\Phi\varepsilon p_5\varepsilon\mu_3 \\ & & & 1 \\ \Phi & \Phi\varepsilon\mu_1 & -\omega_3^2 + \Phi\varepsilon p_5(x_4^2 + \omega_3^2) & -\varepsilon\mu_3(1 - \Phi\varepsilon p_5) \end{bmatrix},$$

$$\mathbf{F}(x_i) = \begin{bmatrix} 0 \\ \Phi\left(\begin{array}{c} \frac{\varepsilon\alpha}{\omega^2}\varepsilon p_2 \sin(x_5) - \frac{\varepsilon\beta}{\omega}\varepsilon p_2 \sin(x_5)x_6 \\ +\varepsilon p_2 x_6^2 \cos(x_5) - \frac{g}{\omega^2}\varepsilon p_2\varepsilon p_4 \sin(x_5)\cos(x_5) \end{array} \right) \\ 0 \\ -\Phi\left(\begin{array}{c} \frac{\varepsilon\alpha}{\omega^2}\varepsilon p_2 \sin(x_5) - \frac{\varepsilon\beta}{\omega}\varepsilon p_2 \sin(x_5)x_6 \\ -\frac{g}{\omega^2}\varepsilon p_2\varepsilon p_4 \sin(x_5)\cos(x_5) + \varepsilon p_2 x_6^2 \cos(x_5) \end{array} \right) \end{bmatrix}, \quad \mathbf{B} = \begin{bmatrix} 0 & 0 \\ 1 & 0 \\ 0 & 0 \\ 0 & 1 \end{bmatrix},$$

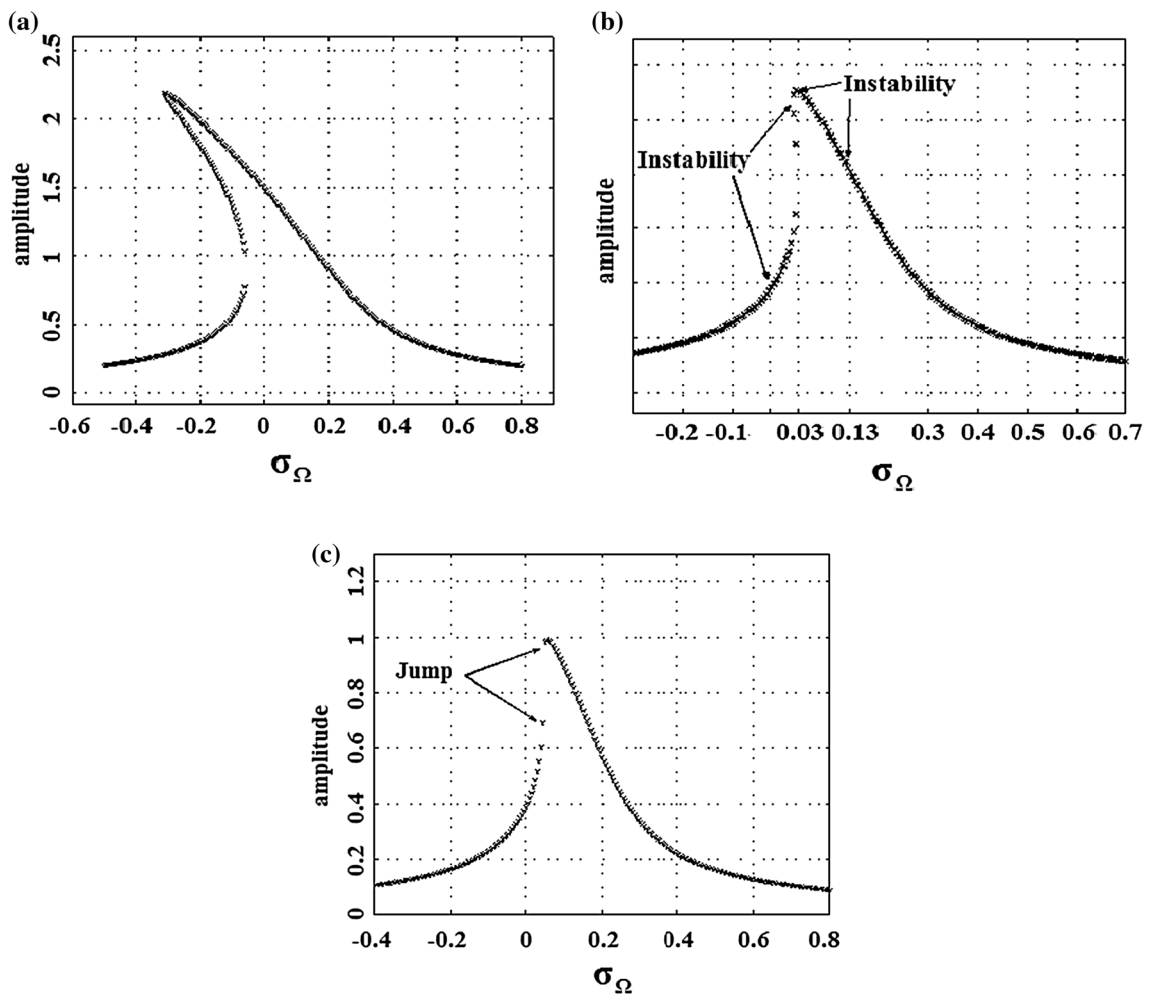J Braz. Soc. Mech. Sci. Eng. (2016) 38:2459–2472

2467

Fig. 4 **a** Frequency–response curve for $\delta < 0$ and $\Omega = 25.3$. **b** Frequency–response curve with $\delta < 0$ and $\Omega = 18$. **c** Frequency-response curve with $\delta < 0$ and $\Omega = 17$

Fig. 5 System (3) and approximation by Eqs. (6) and (7): **a** phase diagram for horizontal displacement. **b** Phase diagram for the angular displacement of the pendulum
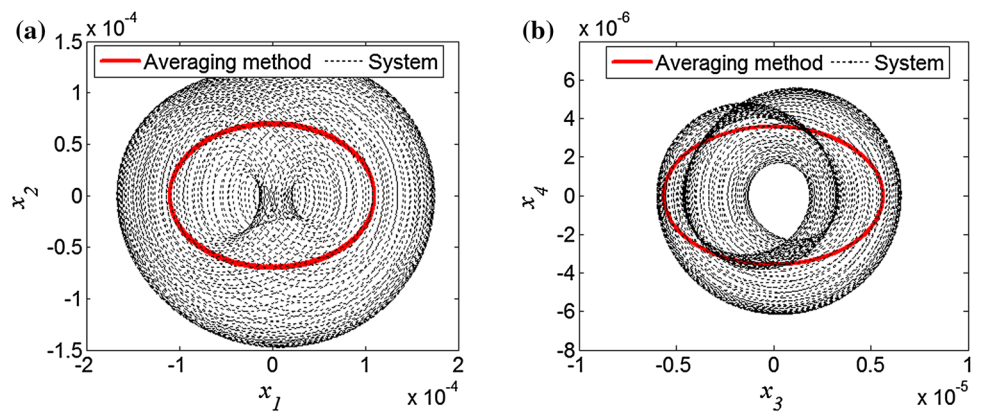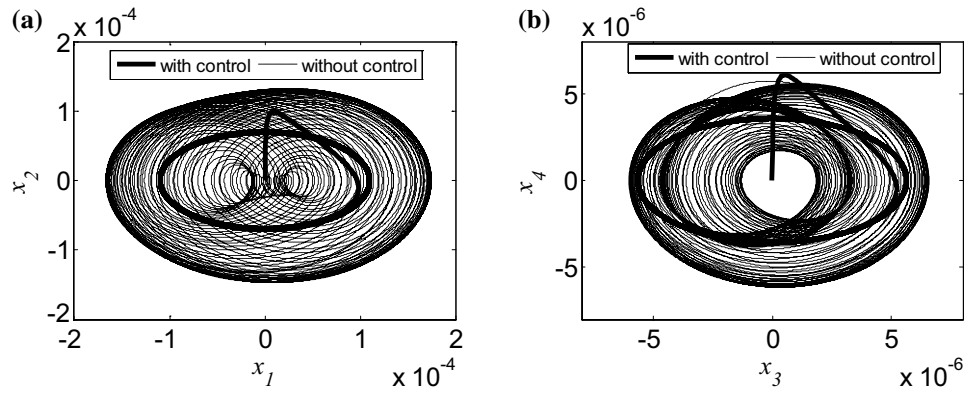
2468

J Braz. Soc. Mech. Sci. Eng. (2016) 38:2459–2472

Fig. 6 System (3) with control: **a** phase diagram for horizontal displacement. **b** Phase diagram for the angular displacement of the pendulum

where: $\Phi = \frac{1}{\varepsilon p_5 - \varepsilon p_2 \varepsilon p_3 \sin(x_5)^2}$, and x_5, x_6 are given by:

$$x_5' = x_6$$

$$
x_6' = \frac{\varepsilon\alpha}{\omega^2} - \frac{\varepsilon\beta}{\omega}x_6 - \frac{\varepsilon p_4 g}{\omega^2}\cos(x_5) + \varepsilon p_3 \sin(x_5)\Phi
$$

$$
\times \begin{pmatrix}
-\varepsilon\mu_1 x_2 - x_1 + \frac{\varepsilon\alpha}{\omega^2}\varepsilon p_2 \sin(x_5) \\
-\varepsilon p_5 x_4^2 x_3 - \varepsilon p_5 \varepsilon\mu_3 x_4 - \varepsilon p_5 \omega_3^2 x_3 \\
-\frac{g}{\omega^2}\varepsilon p_2 \varepsilon p_4 \sin(x_5)\cos(x_5) \\
+\varepsilon p_2 x_6^2 \cos(x_5) - \frac{\varepsilon\beta}{\omega}\varepsilon p_2 \sin(x_5)x_6
\end{pmatrix} \tag{28}
$$

A state feedback instead of output feedback is adopted to improve the control performance. The cost function for the regulator problem is given by:

$$
J_{\text{UF}} = \frac{1}{2}\int_{t_0}^{\infty}\left[\mathbf{y}^T\mathbf{Q}\mathbf{y} + \mathbf{u}_{sf}^T\mathbf{R}\mathbf{u}_{sf}\right]d\tau \tag{29}
$$

where: $\mathbf{y} = \begin{bmatrix} x_1 - x_1^* & x_2 - x_2^* & x_3 - x_3^* & x_4 - x_4^* \end{bmatrix}^T$, x^* are the desired states, $\mathbf{Q}$ is a semi-positive-definite matrix and R positive definite. Assuming full state feedback, the control law is given by:

$$\mathbf{u}_{\text{sf}} = -\mathbf{R}^{-1}\mathbf{B}^T\mathbf{P}_x\mathbf{y} \tag{30}$$

where: $\mathbf{P_x}$ is obtained by the solution of the state-dependent Riccati equation, given by:

$$\mathbf{A}_x^T\mathbf{P_x} + \mathbf{P_x}\mathbf{A_x} - \mathbf{P_x}\mathbf{B_x}\mathbf{R}^{-1}\mathbf{B^T}\mathbf{P_x} + \mathbf{Q} = \mathbf{0} \tag{31}$$

The applied to feedback control (30) implies in the minimization of the functional (29) and in the minimization of the system deviation ($\mathbf{y}$), of the desired state ($\mathbf{x}^*$).

Defining the feedforward control as:

$$
\tilde{u}_{s1} = -\Phi\begin{pmatrix}
\frac{\varepsilon\alpha}{\omega^2}\varepsilon p_2 \sin(x_5) - \frac{\varepsilon\beta}{\omega}\varepsilon p_2 \sin(x_5)x_6 \\
+\varepsilon p_2 x_6^2 \cos(x_5) - \frac{g}{\omega^2}\varepsilon p_2 \varepsilon p_4 \sin(x_5)\cos(x_5)
\end{pmatrix}
$$

$$
\tilde{u}_{s2} = \Phi\begin{pmatrix}
\frac{\varepsilon\alpha}{\omega^2}\varepsilon p_2 \sin(x_5) - \frac{\varepsilon\beta}{\omega}\varepsilon p_2 \sin(x_5)x_6 \\
-\frac{g}{\omega^2}\varepsilon p_2 \varepsilon p_4 \sin(x_5)\cos(x_5) + \varepsilon p_2 x_6^2 \cos(x_5)
\end{pmatrix} \tag{32}
$$

Replacing (32) into (27), the system can be represented in the form:

$$\mathbf{x}' = \mathbf{A_x}\mathbf{x} + \mathbf{B}\mathbf{u}_{sf} \tag{33}$$

5 Numerical simulation of the proposed control

Considering the parameters: $a = 0.05, b = 0.12, m_1 = 3.850$ (kg), $m_2 = 0.008532$ (kg), $m_3 = 0.5$ (kg), $l = 1.19$ (m), $R = 0.075$ (m), $c_1 = 0.0008622$ (N m/s), $c_3 = 0.3234$ (N m/s), $k_1 = 1.75$ (N/m), $\sigma = -0.00099$, $\Omega_1 = 0.1$, $\Omega_f = 55.4$, $a_3 = 0.009$, $J_2 = 0.37$ (kg m^2).

And defining the desired states as (6 and 7):

$$
\begin{aligned}
x_1^* &= a_1 \cos(x_5 + \beta_1) \\
x_2^* &= -a_1\Omega \sin(x_5 + \beta_1) \\
x_3^* &= a_3 \cos(\omega_3\tau + \beta_3) + a_1\delta \cos(x_5 + \beta_1), \\
x_4^* &= -a_3\omega_3 \sin(\omega_3\tau + \beta_3) - a_1\Omega\delta \sin(x_5 + \beta_1)
\end{aligned} \tag{34}
$$

Considering Eqs. (17) the following parameters for (34) are defined as $a_1 = 1.1$, $a_3 = 0$, $\beta_1 = -0.1629\tau$, $\beta_3 = 0$, $\Omega = 0.7416$ and $\delta = 0.0513$.

Defining the matrices: $\mathbf{Q} = 10^3[\mathbf{I}]_{4x4}$ and $\mathbf{R} = [\mathbf{I}]_{2x2}$, the dynamics of the controlled system (27) can be seen in Fig. 6.

It can observed that the proposed control is efficient in taking the states ($\mathbf{x}$) of the system (27) to the desired states $\mathbf{x}^*$ (34).

6 Control system behavior in the presence of parametric errors

To test the effect of parameter uncertainties on the performance of the controller $\mathbf{u}_{\text{sf}}$, the parameters $\varepsilon\mu_1$, εp_5, $\varepsilon\mu_3$ and ω_3 used in matrix ($\mathbf{A}_x$) are considered with a random error of $\pm 20\%$ [21, 27, 28, 30].

In Fig. 7 the variation of system (27) with (control without parametric error) and with (control with parametric error) can be seen, and the SDRE control strategy proved

Fig. 7 Variation of error for u, u', θ and θ' for (control without parametric error) and (control with parametric error)
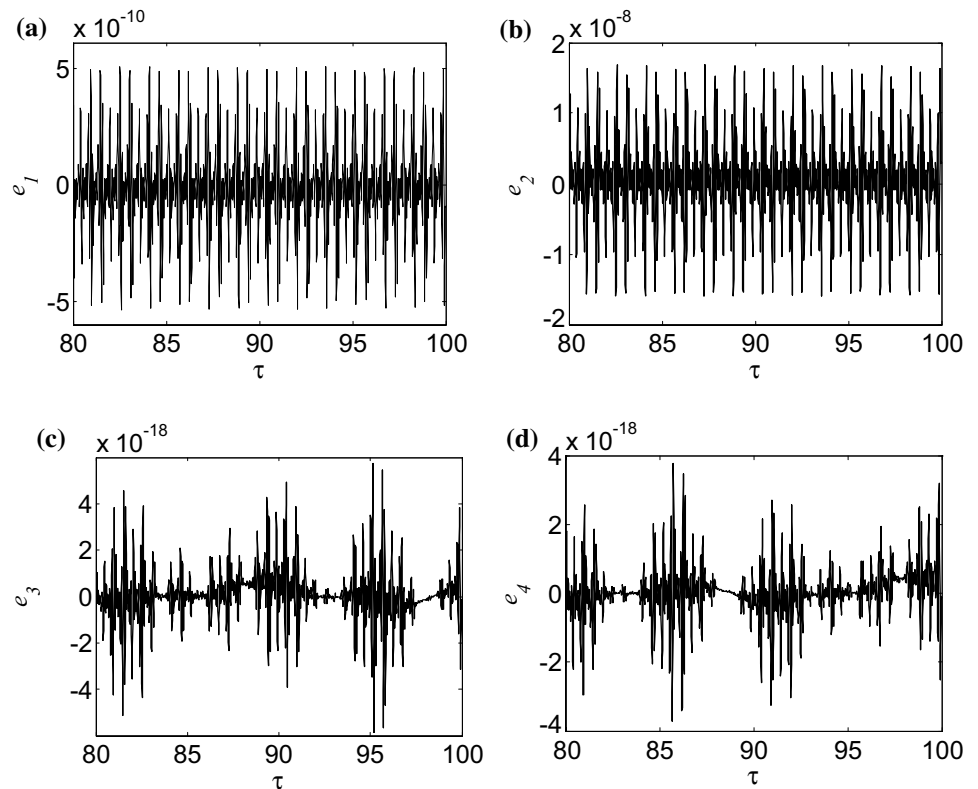
to be robust in the case of parametric variations with errors smaller than (2×10^{-8}).

7 Conclusion

In this work the dynamical behavior of the electro-mechanical pendulum is investigated, applying the SDRE control to synchronize the system motion in a periodic orbit. This system presents complex dynamical effects such as hysteresis, curves of softening and hardening type and Sommerfeld effects. The Routh–Hurwitz criterion is used to determine the steady states stability. Analytical solutions are not feasible due to the complexity of the system's equations. Then some simplifications have been considered enabling the use of average methods [8, 31]. The curves obtained from the frequency response equation show that the electro-mechanical pendulum system presents rich dynamical behavior, exhibiting similar results to that obtained by [8–12, 31]. As it can be seen in Fig. 5a, b, the proposed feedforward control ($\mathbf{u}_{sf}$) and a feedback ($\tilde{\mathbf{u}}_s$) allow to control the oscillations of the electromechanical pendulum system in the periodic orbits obtained by averaging method. Additionally, it can be concluded that the proposed feedback control based on the SDRE method is robust to parametric uncertainties. Similar results are shown in [21, 27, 28, 30]. Showing that the SDRE control strategy is indicated for the electromechanical pendulum control problem.

Appendix

$$J_1 = \frac{a_1'\omega_1}{2\omega_3}\{\cos[(\Omega - \omega_3)\tau + (\beta_1 - \beta_3)] \\ - \cos[(\Omega - \omega_3)\tau + (\beta_1 + \beta_3)]\} \tag{35}$$

$$J_2 = \frac{a_1\beta_1'\omega_1}{2\omega_3}\{\sin[(\Omega + \omega_3)\tau + (\beta_1 + \beta_3)] \\ - \sin[(\Omega - \omega_3)\tau + (\beta_1 - \beta_3)]\} \tag{36}$$

$$J_3 = -\frac{a_3\mu_3}{2}[1 - \cos(2\omega_3\tau + 2\beta_3)] \tag{37}$$

$$J_4 = -\varepsilon\frac{\delta a_1\omega_1\mu_3}{2\omega_3}\{\cos[(\Omega - \omega_3)\tau + (\beta_1 - \beta_3)] \\ - \cos[(\Omega + \omega_3)\tau + (\beta_1 + \beta_3)]\} \tag{38}$$

$$J_5 = -\frac{\delta a_1'\omega_1}{2}\{\cos[(\Omega - \omega_3)\tau + (\beta_1 - \beta_3)] \\ - \cos[(\Omega + \omega_3)\tau + (\beta_1 + \beta_3)]\} \tag{39}$$

$$J_6 = -\frac{\delta a_1\omega_1\beta_1'}{2}\{\sin[(\Omega + \omega_3)\tau + (\beta_1 + \beta_3)] \\ - \sin[(\Omega - \omega_3)\tau + (\beta_1 - \beta_3)]\} \tag{40}$$

$$J_7 = -\frac{\delta a_1}{2}\left(\omega_1\Omega - \Omega_3^2\right)\{\sin[(\Omega+\omega_3)\tau + (\beta_1+\beta_3)] - \sin[(\Omega-\omega_3)\tau + (\beta_1-\beta_3)]\} \tag{41}$$

$$J_1' = \frac{a_1'\omega_1}{2a_3\omega_3}\{\sin[(\Omega+\omega_3)\tau + (\beta_1+\beta_3)] - \cos[(\omega_3-\Omega)\tau + (\beta_3-\beta_1)]\} \tag{42}$$

$$J_2' = \frac{a_1\beta_1'\omega_1}{2a_3\omega_3}\{\cos[(\Omega+\omega_3)\tau + (\beta_1+\beta_3)] + \cos[(\Omega-\omega_3)\tau + (\beta_1-\beta_3)]\} \tag{43}$$

$$J_3' = \frac{a_1\omega_1\Omega}{2a_3\omega_3}\{\cos[(\Omega+\omega_3)\tau + (\beta_1+\beta_3)] + \cos[(\Omega-\omega_3)\tau + (\beta_1-\beta_3)]\} \tag{44}$$

$$J_4' = -\varepsilon\frac{\mu_3}{2}\sin[2(\omega_3\tau + \beta_3)] \tag{45}$$

$$J_5' = -\varepsilon\frac{\mu_3\delta a_1'\omega_1}{2a_3\omega_3}\{\sin[(\Omega+\omega_3)\tau + (\beta_1+\beta_3)] - \sin[(\omega_3-\Omega)\tau + (\beta_3-\beta_1)]\} \tag{46}$$

$$J_6' = -\frac{\delta a_1'\omega_1}{2a_3\omega_3}\{\sin[(\Omega+\omega_3)\tau + (\beta_1+\beta_3)] - \sin[(\omega_3-\Omega)\tau + (\beta_1-\beta_3)]\} \tag{47}$$

$$J_7' = -\frac{\delta a_1\omega_1\beta_1'}{2a_3\omega_3}\{\cos[(\Omega+\omega_3)\tau + (\beta_1+\beta_3)] + \sin[(\Omega-\omega_3)\tau + (\beta_1-\beta_3)]\} \tag{48}$$

$$J_8' = -\frac{\delta a_1}{2a_3\omega_3}\left(\omega_1\Omega - \omega_3^2\right)\{\cos[(\Omega+\omega_3)\tau + (\beta_1+\beta_3)] + \cos[(\Omega-\omega_3)\tau + (\beta_1-\beta_3)]\} \tag{49}$$

$$G_1 = \left(\frac{a_3^2\omega_3^2}{2} + \frac{a_1^2\delta^2 a_3}{4}\right)\{\sin[(2\Omega+2\omega_3)\tau + (\beta_1+3\beta_3)] - \sin[(\omega_3-\Omega)\tau + (\beta_3-\beta_1)]\} \tag{50}$$

$$G_2 = \left(-\frac{a_3^2\omega_3^2}{2}\right)\{\sin[(\Omega+3\omega_3)\tau + (\beta_1+3\beta_3)] - \sin[(3\omega_3-\Omega)\tau + (3\beta_3-\beta_1)]\} \tag{51}$$

$$G_3 = \left(-\frac{a_3^2\omega_3 a_1\delta}{4}\right)\{\sin[(2\Omega+2\omega_3)\tau + (2\beta_1+2\beta_3)] - \sin(2\omega_3\tau + 2\beta_3)\} \tag{52}$$

$$G_4 = \left(-\frac{a_1^2\delta^3}{8}\right)\{\sin[(3\Omega+\omega_3)\tau + (3\beta_1+\beta_3)] - \sin[(\Omega+\omega_3)\tau + (\beta_3+\beta_1)]\} \tag{53}$$

$$G_5 = \left(-\frac{a_1^2\delta^2 a_3}{8}\right)\{\sin[(3\Omega-\omega_3)\tau + (3\beta_1-\beta_3)] - \sin[(\Omega-\omega_3)\tau + (\beta_1-\beta_3)]\} \tag{54}$$

$$G_6 = \left(\frac{a_3^2\omega_3^2 a_1\delta}{4} + \frac{a_3^2\delta^2}{2} - \frac{a_1^3\delta^3}{8}\right)[\sin(2\Omega\tau + 2\beta_1)] \tag{55}$$

$$G_7 = \left(-\frac{a_3^2\omega_3^2\delta a_1}{8}\right)\{\sin[(2\Omega+2\omega_3)\tau + (2\beta_1+2\beta_3)] - \sin(2\omega_3\tau + 2\beta_3)\} \tag{56}$$

$$G_8 = \left(-\frac{a_3^2\omega_3^2\delta a_1}{8}\right)\{\sin(2\omega_3\tau + 2\beta_3) - \sin[(2\omega_3-2\Omega)\tau + (2\beta_3-2\beta_1)]\} \tag{57}$$

$$G_9 = \left(\frac{a_1^2\delta^2 a_3\omega_3}{4}\right)\{\sin[(3\Omega-\omega_3)\tau + (3\beta_1-\beta_3)] - \sin[(\Omega-\omega_3)\tau + (\beta_1-\beta_3)]\} \tag{58}$$

$$G_{10} = \left(-\frac{a_1^2\delta a_3\omega_3}{4}\right)\{\sin[(3\Omega+\omega_3)\tau + (3\beta_1+\beta_3)] - \sin[(\Omega+\omega_3)\tau + (\beta_1+\beta_3)]\} \tag{59}$$

$$G_{11} = \left(\frac{a_1\delta a_3\omega_3}{8}\right)\{\sin(4\Omega\tau + 4\beta_1) - \sin(2\Omega\tau + 2\beta_1)\} \tag{60}$$

$$G_{12} = \left(\frac{a_3'\omega_3}{2}\right)\{\cos[(\omega_3-\Omega+)\tau + (\beta_3-\beta_1)] - \sin[(\omega_3-\Omega)\tau + (\beta_3-\beta_1)]\} \tag{61}$$

$$G_{13} = \left(\frac{a_3\omega_3\beta_3'}{2}\right)\{\sin[(\omega_3+\Omega)\tau + (\beta_3+\beta_1)] - \sin[(\omega_3-\Omega)\tau + (\beta_3-\beta_1)]\} \tag{62}$$

$$G_{14} = \left(\frac{a_3\omega_3^2}{2}\right)\{\sin\left[(\omega_3 + \Omega)\tau + (\beta_3 + \beta_1)\right]$$
$$- \sin\left[(\omega_3 - \Omega)\tau + (\beta_3 - \beta_1)\right]\} \tag{63}$$

$$G_1' = \left(\frac{a_3^3\omega_3^2}{4} - \frac{a_3^3\omega_3^3}{8} + \frac{a_1^2\delta^2\omega_1^2 a_3}{4}\right)\{\cos\left[(\Omega + \omega_3)\tau + (\beta_1 + \beta_3)\right]\} \tag{64}$$

$$G_2' = \left(-\frac{a_3^3\omega_3^2}{4}\right)\{\cos\left[(3\omega_3 + \Omega)\tau + (3\beta_3 + \beta_1)\right]$$
$$+ \cos\left[(3\omega_3 - \Omega)\tau + (3\beta_3 - \beta_1)\right]\} \tag{65}$$

$$G_3' = \left(\frac{a_3^2\omega_3 a_1\delta}{4}\right)\left\{\begin{array}{l}[\cos(2\omega_3\tau) + \cos(2\omega_3 - 2\Omega)\tau + (2\beta_3 - 2\beta_1)] \\ -[\cos\left[(2\omega_3 + 2\Omega)\tau + (3\beta_3 + 2\beta_1)\right] + \cos(2\omega_3\tau + 2\beta_3)]\end{array}\right\} \tag{66}$$

$$G_4' = \left(-\frac{a_1^2\omega_1^3 a_3\delta^2}{8}\right)\left\{\begin{array}{l}[\cos((3\Omega + \omega_3)\tau + (3\beta_1 + \beta_3)) + \cos((\Omega + \omega_3)\tau)] \\ +[\cos\left[(2\Omega - \omega_3)\tau + (3\beta_1 - \beta_3)\right] + \cos\left[(\Omega - \omega_3)\tau + (\beta_1 - \beta_3)\right]]\end{array}\right\} \tag{67}$$

$$G_5' = \left(\frac{a_3^2\omega_3 a_1\delta}{4} + \frac{a_3^3\omega_1^2\delta^3}{4} - \frac{a_1^3\delta^3\omega_1^2}{8}\right)\left[1 - \cos(2\Omega\tau + 2\beta_1)\right] \tag{68}$$

$$G_6' = \left(-\frac{a_3^2\omega_3^2 a_1\delta}{8}\right)\left\{\begin{array}{l}[\cos((2\Omega + \omega_3)\tau + (2\beta_1 + 2\beta_3)) + \cos(2\omega_3\tau + 2\beta_3)] \\ +[\cos(2\omega_3\tau + 2\beta_3) + \cos\left[(2\omega_3 - 2\Omega)\tau + (2\beta_3 - 2\beta_1)\right]]\end{array}\right\} \tag{69}$$

$$G_7' = \left(\frac{a_1^2\omega_3^2 a_3\delta}{4}\right)\left\{\begin{array}{l}[\cos((3\Omega - \omega_3)\tau + (3\beta_1 - \beta_3)) + \cos((\Omega - \omega_3)\tau + (\beta_1 - \beta_3))] \\ -[\cos((\omega_3 + 3\Omega)\tau + (3\beta_1 + \beta_3)) + \cos\left[(\omega_3 + \Omega)\tau + (\beta_3 + \beta_1)\right]]\end{array}\right\} \tag{70}$$

$$G_8' = \left(-\frac{a_3^3\omega_1^2\delta^3}{8}\right)\left[\cos(4\Omega\tau + 4\beta_1) + \cos(2\Omega\tau + 2\beta_1)\right]$$
$$+ \left(\frac{a_3'\omega_3}{2}\right)\left[\sin((\Omega + \omega_3)\tau + (\beta_1 + \beta_3))\right.$$
$$\left. - \sin((\Omega - \omega_3)\tau + (\beta_1 - \beta_3))\right] \tag{71}$$

$$G_9' = \left(\frac{a_3\omega_3\beta_3'}{2}\right)\{\cos\left[(\Omega + \omega_3)\tau + (\beta_3 + \beta_1)\right]$$
$$+ \cos\left[(\omega_3 - \Omega)\tau + (\beta_3 - \beta_1)\right]\} \tag{72}$$

$$G_{10}' = \left(\frac{a_3\omega_3^2}{2}\right)\{\cos\left[(\Omega + \omega_3)\tau + (\beta_3 + \beta_1)\right]$$
$$+ \cos\left[(\omega_3 - \Omega)\tau + (\beta_3 - \beta_1)\right]\} \tag{73}$$

References

1. Kononenko VO (1969) Vibrating systems with a limited power supply. Iliffe Books Ltd, London
2. Nayfeh AH (1981) Introduction to Perturbation Techniques. John Wiley & Sons Inc, New York
3. Danuta S, Kot M (2007) Chaotic vibration of an autoparametrical system with a non-ideal source of power. J Theor Appl Mech 45(1):119–131
4. Balthazar JM, Mook DT, Weber HI, Brasil RMLRF, Fenili A, Belato D, Felix JLP (2001) Recent results on vibrating problems with limited power supply. In: Sixth Conference on dynamical Systems Theory and Applications, Lodz, Poland, December, 10–12, 27–50
5. Gonçalves PJP, Silveira M, Pontes Junior BR, Balthazar JM (2014) The dynamic behavior of a cantilever beam coupled to a non-ideal unbalanced motor through numerical and experimental analysis. J Sound Vib 333:5115–5129
6. Cveticanin L, Zukovic M (2015) Motion of a motor-structure non-ideal system. Eur J Mech A Solids 53:229–240
7. Fossi DOT, Woafo P (2013) Generation of complex phenomena in a simple electromechanical system using the feedback control. Commun Nonlinear Sci Numer Simulat 18:209–218
8. Palacios JL, Balthazar JM, Brasil RMLRF (2002) On nonideal and nonlinear portal frame dynamics analysis using bogoliubov averaging method. J Braz Soc Mech Sci Eng 24(4):257–265
9. Felix JLP, Balthazar JM, Brasil RMLRF (2005) On saturation control of a non-ideal vibrating portal frame foundation type shear-building. J Vib Control 11:121–136
10. Arbex HC, Balthazar JM, Pontes BR Jr, Brasil RMLRF, Felix JLP, Tusset AM, Bueno AM (2015) On nonlinear dynamics behavior and control of a new model of a magnetically levitated vibrating system, excited by an unbalanced DC motor of limited power supply. J Braz Soc Mech Sci Eng 37(4):1139–1150
11. Piccirillo V, Tusset AM, Balthazar JM (2014) Dynamical jump attenuation in a non-ideal system through magneto rheological damper. J Theor Appl Mech (Warsaw) 53:595–604

2472

J Braz. Soc. Mech. Sci. Eng. (2016) 38:2459–2472

12. Djanan AAN, Nbendjo BRN, Woafo P (2013) Electromechanical control of vibration on a plate submitted to anon-ideal excitation. Mech Res Commun 54:72–82

13. Tusset AM, Balthazar JM, Felix JLP (2013) On elimination of chaotic behavior in a non-ideal portal frame structural system, using both passive and active controls. J Vib Control 19(6):803–813

14. Pearson JD (1962) Approximation methods in optimal control. J Electron Control 13:453–469

15. Wernli A, Cook G (1975) Suboptimal control for the nonlinear quadratic regulator problem. Automatica 11:75–84

16. Mracek CP, Cloutier JR (1998) Control designs for the nonlinear benchmark problem via the state-dependent Riccati equation method. Int J Robust Nonlinear Control 8:401–433

17. Friedland B (1996) Advanced control system design. Prentice-Hall, Englewood Cliff, pp 110–112

18. Balthazar JM, Bassinello DG, Tusset AM, Bueno AM, Pontes BR (2014) Nonlinear control in an electromechanical transducer with chaotic behavior. Meccanica 49(8):1859–1867

19. Tusset AM, Balthazar JM (2013) On the chaotic suppression of both ideal and non-ideal duffing based vibrating systems, using a magnetorheological damper. Differ Equ Dyn Syst 21:105–121

20. Bueno AM, Tusset AM, Santos JPM, Ttsushida M, Balthazar JM (2013) SDRE control applied to an electromechanical pendulum excited by a non-ideal motor. In: Proceedings of the ASME 2013 International Design Engineering Technical Conferences & Computers and Information in Engineering Conference IDETC/CIE 2013, August 4–7, Portland, Oregon, USA, 2013

21. Tusset MA, Piccirillo V, Bueno AM, Balthazar MJ, Sado D, Felix JLP, Brasil RMLRDF (2015) Chaos control and sensitivity analysis of a double pendulum arm excited by an RLC circuit based nonlinear shaker. J Vib Control 1:1–17

22. Molter A, Silveira OAA, Fonseca JSO, Bottega V (2010) Simultaneous piezoelectric actuator and sensor placement optimization and control design of manipulators with flexible links using SDRE method. Math Problems Eng 2010:362437

23. Fenili A, Balthazar JM (2011) The rigid-flexible nonlinear robotic manipulator: modeling and control. Commun Nonlinear Sci Numer Simul 16(5):2332–2341

24. Lima JJ, Tusset AM, Janzen FC, Piccirillo V, Nascimento CB, Balthazar JM, Brasil MRLF (2014) Nonlinear state estimation and control applied to a manipulator robotic including drive motor. Math Eng Sci Aerosp Transdiscipl Int J 5:413–425

25. Tusset AM, Balthazar JM, Bassinello DG, Pontes BR, Felix JLP (2012) Statements on chaos control designs, including a fractional order dynamical system, applied to a MEMS comb-drive actuator. Nonlinear Dyn 69:1837–1857

26. Tusset AM, Bueno AM, Nascimento CB, Kaster MS, Balthazar JM (2013) Nonlinear state estimation and control for chaos suppression in MEMS resonator. Shock Vib 20:749–761

27. Balthazar JM, Tusset AM, Souza SLTD, Bueno AM (2012) Microcantilever chaotic motion suppression in tapping mode atomic force microscope. Proc Inst Mech Eng Part C J Mech Eng Sci 227:1730–1741

28. Nozaki R, Balthazar JM, Tusset AM, Pontes BR, Bueno AM (2013) Nonlinear control system applied to atomic force microscope including parametric errors. J Control Autom Electri Syst 24:223–231

29. Rodrigues KS, Balthazar JM, Tusset AM, Pontes BR, Bueno AM (2014) Preventing chaotic motion in tapping-mode atomic force microscope. J Control Autom Electri Syst 25:732–740

30. Balthazar JM, Tusset AM, Bueno AM (2014) Nonlinear TM-AFM control considering parametric errors in the control signal evaluation. J Theor Appl Mech (Warsaw) 52:93–106

31. Felix JLP, Balthazar JM, Brasil RMLRF (2009) Comments on nonlinear dynamics of a non-ideal Duffing–Rayleigh oscillator: numerical and analytical approachs. J Sound Vib 319:1136–1149

32. El-Badawy AA (2007) Behavioral investigation of a nonlinear vibrating system. J Vib Control 13(2):203–217

33. Kuo BC (1995) Automatic control systems. Prentice Hall, New Jersey